
A Simple and Efficient Baseline for Data Attribution on Images

Vasu Singla¹ Pedro Sandoval-Segura¹ Micah Goldblum²
Jonas Geiping³ Tom Goldstein¹

¹University of Maryland ²New York University

³ ELLIS Institute Tübingen, MPI for Intelligent Systems, Tübingen AI Center
{vsingla, psando, tomg}@cs.umd.edu jonas@tue.ellis.edu goldblum@nyu.edu

Abstract

Data attribution methods play a crucial role in understanding machine learning models, providing insight into which training data points are most responsible for model outputs during deployment. However, current state-of-the-art approaches require a large ensemble of as many as 300,000 models to accurately attribute model predictions. These approaches therefore come at a high computational cost, are memory intensive, and are hard to scale to large models or datasets. In this work, we focus on a minimalist baseline that relies on the image features from a pretrained self-supervised backbone to retrieve images from the dataset. Our method is model-agnostic and scales easily to large datasets. We show results on CIFAR-10 and ImageNet, achieving strong performance that rivals or outperforms state-of-the-art approaches at a fraction of the compute or memory cost. Contrary to prior work, our results reinforce the intuition that a model’s prediction on one image is most impacted by visually similar training samples. Our approach serves as a simple and efficient baseline for data attribution on images.

1 Introduction

The effectiveness of a machine learning system’s performance hinges on the quality, diversity, and relevance of the data it is trained on (Halevy et al., 2009; Sun et al., 2017). In various real-world machine learning systems, for example in healthcare or finance, we often ask questions like, “Which training samples influenced this prediction?” or “How sensitive is this model’s prediction to changes in the training data?” Counterfactual insights enable us to assess the impact of hypothetical changes in the data distribution, which in turn helps us understand the basis of the model’s decisions and how to change the decision in the event of an error.

These questions motivate research on *data attribution* methods, which focus on understanding which data points most strongly influence a model’s outputs. Data attribution methods have been applied to applications such as debugging model biases (Ilyas et al., 2022; Park et al., 2023; Shah et al., 2023), fairness assessment (Black & Fredrikson, 2021), and active learning (Liu et al., 2021).

In principle, data attribution can be done perfectly by a brute-force leave- k -out strategy; simply train the model from scratch many times, removing k data points each time. The user can then examine the impact of each data point by examining how the corresponding ablated model differs from the original. Clearly, this procedure is intractable for any realistic problem as there are innumerable subsets, and training even a single machine learning model can be almost prohibitively expensive. The goal of data attribution research therefore is to approximate this gold standard metric as closely as possible while simultaneously using as little computation as possible. As such, the field of data attribution is all about trade-offs between accuracy, runtime, and memory.

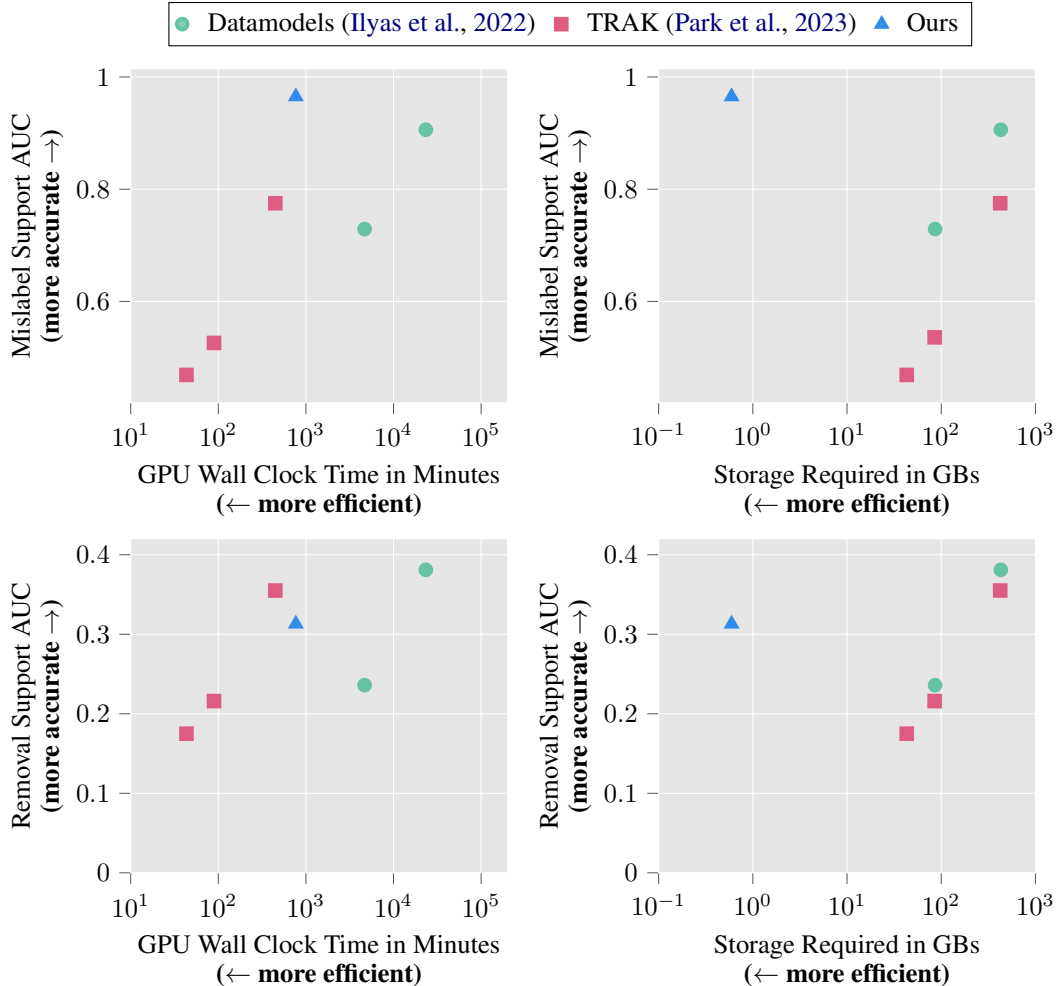


Figure 1: **Our proposed baseline approach for data attribution achieves high performance while improving computational efficiency and storage requirements.** The wall clock time is computed on an RTX A6000 GPU and memory requirements is computed in GBs (see Appendix A.1). Mislabeled and Removal Support AUC are used to measure the method’s accuracy to make counterfactual predictions (see details in Section 2.1).

Existing data attribution approaches gain insights into model behaviors by scraping information from the learning algorithm, such as logits (Ilyas et al., 2022) or gradients (Koh & Liang, 2017; Park et al., 2023). Despite this, these techniques still require re-training multiple models on different data subsets, or other compute and memory intensive strategies for better efficacy (Ilyas et al., 2022; Feldman & Zhang, 2020; Koh & Liang, 2017; Park et al., 2023). Current data attribution approaches quickly become intractable as datasets become larger (Basu et al., 2021; Park et al., 2023) and applications become more realistic, such as attribution for LLMs (Grosse et al., 2023).

In this work, we present a simple approach that outperforms the current state of the art in terms of compute-accuracy trade-offs, and often in terms of raw performance numbers as well. Given a test image, we use the feature space of a single self-supervised model to retrieve similar images, revealing a compelling association between data attribution and *visual similarity*. In contrast to existing methods that involve unwieldy model ensembles and extensive computation, our approach shifts the spotlight directly onto the data. Building on prior research, we focus on counterfactual prediction (Ilyas et al., 2022; Park et al., 2023) for evaluating data attribution techniques. Based on the intuition that data inherently shapes model behavior, our method does not use any information about the model training process, and yet still rivals the performance of state-of-the-art approaches

that do, while using a tiny fraction of the computational resources. Our work shows that contrary to previous work (Ilyas et al., 2022; Park et al., 2023), feature representations can serve as a robust baseline for data attribution methods. Our code is available at <https://github.com/vasusingla/simple-data-attribution>

2 Problem Setting

We first define our notation and then discuss evaluation criteria used for data attribution approaches. We borrow notation and evaluation criteria from Ilyas et al. (2022) and Park et al. (2023).

Notation: Let $S = \{z_1, z_2, \dots, z_n\}$ denote a set of training samples. Each sample $z_i \in S$ represents $z_i = (x_i, y_i)$, where x_i signifies the input image and y_i represents the associated ground truth label. We use z_t to denote an arbitrary evaluation sample not present in the training set.

We denote a data attribution approach as a function $\tau(z, S) \in \mathbb{R}^n$. This function operates on any sample z and a training set S , generating a score for each sample within the set S . These scores highlight the relative positive or negative impact of individual training samples on the classification of the input sample z .

2.1 Evaluating Attribution Methods

Obtaining ground truth for data attribution has been a challenging problem. Several works have focused on evaluating data attribution methods using alternatives such as Shapley values or leave-one-out influences (Koh & Liang, 2017; Lundberg & Lee, 2017; Jia et al., 2021). These approaches however do not scale beyond modest dataset sizes. An alternate line of work evaluates the utility of attribution methods for auxiliary tasks such as active learning or identifying mislabeled or poisoned data samples (Liu et al., 2021; Jia et al., 2021).

Recent research primarily concentrates on evaluating the performance of data attribution methods through the lens of their capacity to provide accurate counterfactual predictions (Park et al., 2023; Ilyas et al., 2022). While these metrics can be computationally demanding, they represent a straightforward, yet valuable, proxy for assessing the effectiveness of attribution approaches. In our work, we replicate the approach presented in Ilyas et al. (2022) and focus on **data brittleness**. Data brittleness metrics leverage attribution techniques to answer the following question: “*To what extent are model predictions sensitive to modifications in the training data?*” Hence, these metrics serve as a means of estimating counterfactual scenarios. To quantify data brittleness, we focus on two distinct types of data support for a validation sample z_t . We explain these below:

Data Removal Support: The smallest subset R_r , that when removed from the training set S , causes an average training run of the model to misclassify z_t .

Data Mislabel Support: The smallest training subset R_m , whose mislabeling causes an average training run of the model to misclassify z_t . For each training sample in R_m , we change the labels to the second-highest predicted class for z_t .

Intuitively, a better data attribution approach should be able to find a smaller subset of training samples that can misclassify z_t . We estimate these metrics over a set of validation samples and plot the cumulative distribution (CDF), which represents the probability that a sample’s label can be flipped as a function of the data subset size. In Section 1, we compare the Area Under Curve (AUC) of the CDF for the metrics described above across our approach and other attribution methods.

For a validation sample z_t and a data attribution approach $\tau(z, S)$, we rank the training samples based on decreasing order of positive influence on z_t . Then, based on the ranking, we iteratively select and modify a subset of training data. We perform this search, over different subsets to compute the smallest training subset that can cause z_t to be misclassified. Naively, checking all possible subsets would be computationally expensive. Ilyas et al. (2022) check only subsets with certain discrete sizes to keep costs manageable. We instead propose to perform a **bisection search** to approximate the search for the smallest subset, yielding more accurate results. The bisection search approximation is supported by the observation that several data attribution approaches are additive (Park et al., 2023). The exact algorithm and details are discussed in Appendix A.5.

Linear Datamodeling Score (LDS) is another related metric used for the evaluation of data attribution methods (Ilyas et al., 2022; Park et al., 2023). Note that the LDS metric focuses on counterfactual predictions for *arbitrary* changes in training data. In contrast, data brittleness serves to quantify the accuracy of counterfactual predictions using *targeted* changes to training data based on a specific validation sample. Thus, the latter metric serves as a better proxy for the data attribution method’s usefulness as a debugging tool. In this work, we emphasize performance on data brittleness and provide results for the LDS metric in Appendix A.6.

3 Our Approach & Baselines

Our approach utilizes the feature space of a neural network to extract features from a validation sample z_t and each training sample in S . We then compute the attribution scores by measuring the distance in feature space between z_t and each training sample in S . Prior works have tried similar approaches and claimed them to be ineffective for counterfactual estimation (Park et al., 2023; Ilyas et al., 2022). In the next sections, we describe the details of our approach and discuss our baselines.

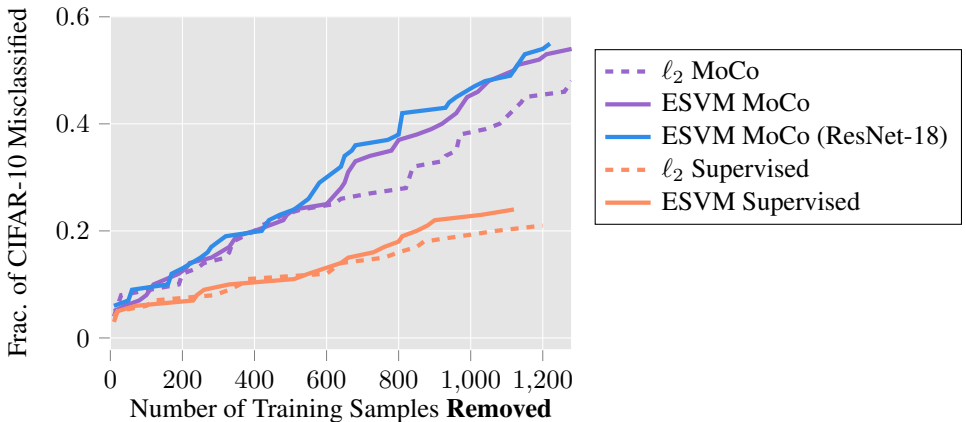


Figure 2: **Self-supervised features are more effective than supervised and are best compared using an ESVM.** Self-supervised features from MoCo can be used to find smaller data support than standard supervised features. For a larger fraction of test samples, ESVM distance is more effective than ℓ_2 distance at ranking train images to select smaller data removal support.

3.1 Design Choices

Our data attribution approach relies on the comparison of image embeddings, and in doing so, we make decisions regarding the choice of feature extractor, the subset of training images to compare, and the distance function.

Feature extractor. We find that the learning paradigm used to train a feature extractor heavily influences the estimation of data support. For example, embeddings from a ResNet-9 trained using a self-supervised learning objective (MoCo, (He et al., 2020)) can be used to find smaller support sets than the same model trained in a supervised manner (See ℓ_2 MoCo vs ℓ_2 Supervised in Fig. 2). With the exception of DINO (Caron et al., 2021), all self-supervised feature extractors perform better than their supervised counterpart (see Appendix A.2 Fig. 8). We found that MoCo features outperform other self-supervised approaches in both data removal support and mislabeling support scenarios, leading us to select a MoCo model as our preferred feature extractor. We find that the ResNet-18 backbone provides better support estimates than ResNet-9, and hence use it as default for all our experiments.

Subset of train images. In Appendix A.3 Fig. 11, we show that choosing a support set from training images of class the same class y as the target $z_t = (x, y)$ is critical, *i.e.* given a target image of an airplane, we only rank airplane training images.

Distance function. When measuring the distance between two embeddings, Euclidean distance (ℓ_2) is a common choice (Ilyas et al., 2022; Park et al., 2023). Cosine distance and Mahalanobis distance

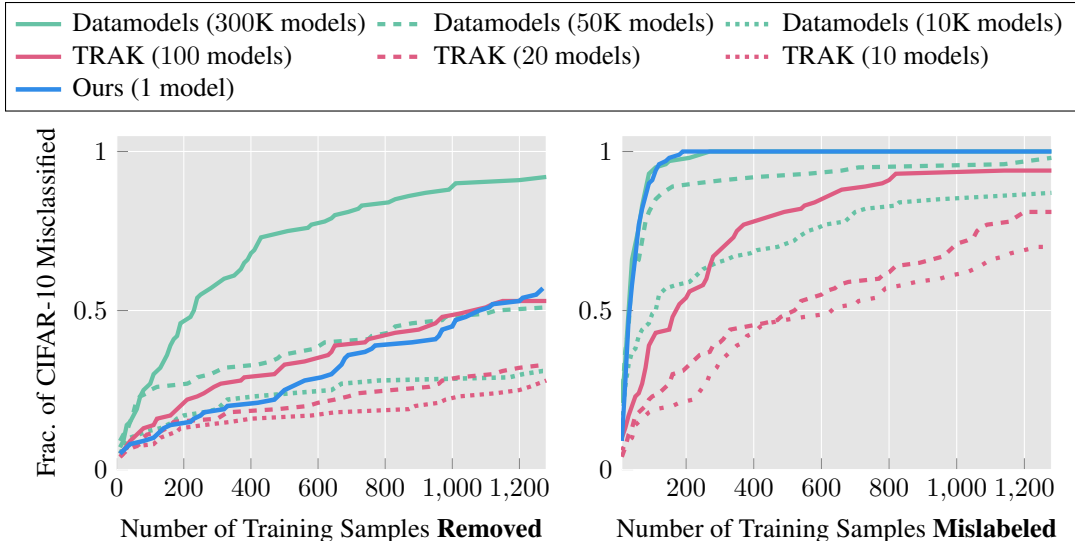


Figure 3: **Our baseline approach uses only a single model and outperforms TRAK and Datamodels using 20 and 10,000 models for data brittleness metrics.** We estimate data removal and data mislabel support for 100 random CIFAR-10 test samples using a ResNet-9 model and plot the cumulative distribution using our approach and other baselines. The number of models used by each approach is also shown. For data removal support, using only a single model our proposed approach outperforms TRAK (Park et al., 2023) using 20 models and Datamodels (Ilyas et al., 2022) using 10,000 models. For data mislabel support, we outperform TRAK using 100 models and perform equivalent to Datamodels using 300,000 models.

have also been used to measure similarity, but these were found to perform similarly to Euclidean distances in previous work (Hanawa et al., 2021; Ilyas et al., 2022; Park et al., 2023).

However, we find that measuring distance as distance to the hyperplane of an Exemplar SVM (ESVM) improves image similarity (Malisiewicz et al., 2011). To compute this metric, we train a linear SVM using one positive sample (the target embedding) and treat all other samples (the remaining embeddings of the same class) as negative samples. In this way, the decision boundary, and consequently the distance function, is defined largely by unique dimensions of the target with respect to all embeddings of the same class. In Fig. 2, we demonstrate how using distance to the hyperplane of an ESVM yields better removal support estimates than ℓ_2 distance.

3.2 Baselines

Datamodels (Ilyas et al., 2022): In the *Datamodeling* framework, the end-to-end training and evaluation of deep neural networks is approximated with a parametric function. Surprisingly, optimizing a linear function is enough to predict model outputs reasonably well, when given a training data subset. By collecting a large dataset of subset-output pairs, Ilyas et al. (2022) demonstrate that such a linear mapping can accurately predict the correct-class margin. Among other use-cases, these Datamodels are shown to be effective at counterfactual predictions and identifying visually similar train-test samples. But Datamodeling is prohibitively expensive, requiring the training of hundreds of thousands of models (300,000 in the original work) to generate optimal subset-output data. Unfortunately, this limitation makes Datamodeling intractable for all but small toy problems.

TRAK (Park et al., 2023): By approximating models with a kernel machine, *Tracing with the Randomly-projected After Kernels* (TRAK) makes progress toward reducing the computational cost of data attribution by reducing dimensionality with random projections and ensembling over independently trained models. However, the method tends to only work well with more than a dozen model checkpoints and a large projection dimension for the model gradients, the storage of which can surpass 80GB when using a ResNet-9 on CIFAR-10. Compared to Datamodels, TRAK gains in runtime are paid for in storage space.

4 Counterfactual Estimation

We evaluate these approaches and our proposed baseline data attribution for a number of classification examples in computer vision, focusing on datasets such as CIFAR-10 and ImageNet, which are small enough to allow for some comparison with the more expensive approaches of TRAK and Datamodels.

4.1 Experimental Setup

Training Setup: We estimate the approximate data removal and data mislabel support for CIFAR-10 and ImageNet. As computing the data support for even a single validation sample requires training multiple models, we restrict ourselves to a reasonably small set of validation samples. We use the same validation samples across all attribution methods. To accelerate the training of these models, we use the FFCV library (Leclerc et al., 2023).

For CIFAR-10 (Krizhevsky et al., 2009), we train ResNet-9¹ and MobileNetV2 (Sandler et al., 2018) models for 24 epochs using a batch size of 512, momentum of 0.9, label smoothing of 0.1, with a cyclic learning schedule, with a maximum value of 0.5. The test accuracy for these models without any modification to training data is above 92%. We randomly selected 100 validation samples, in a class-balanced manner for our brittleness metrics. We remove or mislabel a maximum of 1280 training samples for each validation sample. Our training setup is similar to Ilyas et al. (2022).

For ImageNet (Deng et al., 2009), we train ResNet-18 (He et al., 2015) models for 16 epochs, using a batch size of 1024. We train on 160×160 resolution images for the first 11 epochs and increase the training resolution to 192×192 for the last 5 epochs. The other hyperparameters are kept the same as CIFAR-10. These models achieve a top-1 validation accuracy of 67%. We randomly selected 30 validation samples, from a subset of validation samples that are not misclassified by 4 ResNet-18 models on average. We removed or mislabeled a maximum of 1000 training samples for each validation sample.

Baselines and Our Setup: To estimate TRAK scores on CIFAR-10, we train 100 ResNet-9 models and use a projection dimension of 20480. To estimate scores on ImageNet, we train 4 ResNet-18 models and use a projection dimension of 4096. Computing TRAK scores using 4 models already requires 160 GB of storage space, hence we refrain from using a larger ensemble of models.

For Datamodels, we download the pre-trained weights optimized using outputs from 300K ResNet-9 models with 50% random subsets.² We also download the binary masks and margins to train our own Datamodels on outputs from 10K and 50K ResNet-9 models, using another 10K models for validation. Since Datamodels are extremely compute-intensive and require training hundreds of thousands of models, we cannot include them as a baseline on ImageNet.

For our baseline approach to train self-supervised models, we use the Lightly library (Susmelj et al., 2020). We train a ResNet-18 model using MoCo (He et al., 2020) for 800 epochs on CIFAR-10, using the Lightly benchmark code.³ On ImageNet, we download a pre-trained ResNet-50 model trained using MoCo.⁴ For our approach, we always use a single model. We denote Datamodels using N models as Datamodels (N), and similarly for TRAK.

4.2 CIFAR-10 Data Brittleness

In Fig. 3, we present the distribution of estimated data removal values for CIFAR-10. Our findings reveal that employing a single model with a MoCo backbone (He et al., 2020) for data removal support proves more effective than employing Datamodels with 10,000 models and TRAK with 20 models. Our approach and Datamodels (10K) identify that 23% samples can be misclassified by removing fewer than 500 (example-specific) training samples while TRAK (20) can only identify 16%. For support sizes up to 1280 images, our approach identifies 55% of validation samples, whereas TRAK (20) and Datamodels (10K) can only identify 28% and 31% samples respectively.

¹<https://github.com/wbaek/torchskeleton/blob/master/bin/dawnbench/cifar10.py>

²<https://github.com/MadryLab/datamodels-data>

³https://docs.lightly.ai/self-supervised-learning/getting_started/benchmarks.html

⁴<https://github.com/facebookresearch/moco>

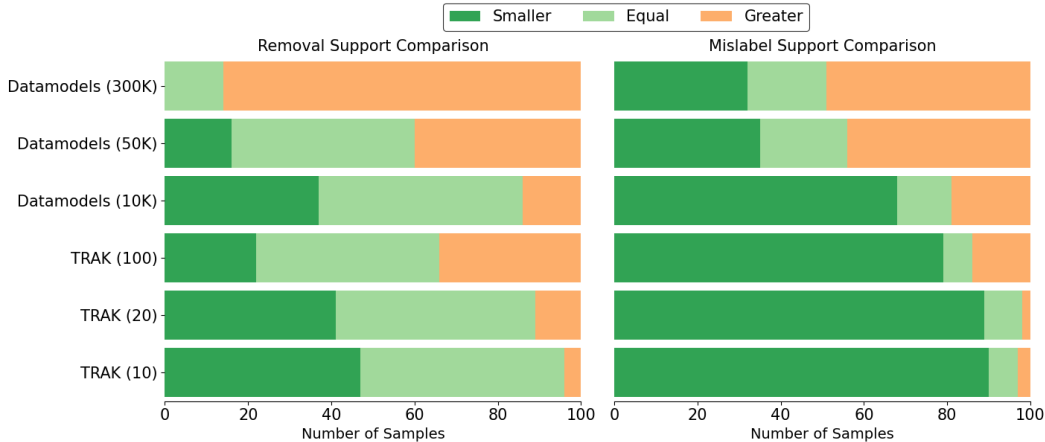


Figure 4: Compared to instances of Datamodels and TRAK, we check whether our data support estimates are smaller, equal, or larger for all 100 validation samples. For 32 samples, our proposed method can find smaller data mislabel support compared to Datamodels (300k models). Even for the data removal case, our approach can find an equivalent support estimate to Datamodels (300k models) for 14 samples.

In the same figure, we also depict the distribution of estimated data mislabel support for CIFAR-10. Here, our approach outperforms TRAK (100) and approaches the performance of Datamodels (300K). Here, our approach identifies 47% of CIFAR-10 validation samples that can be misclassified by mislabeling less than 30 training samples! In contrast, TRAK (100) performs poorly identifying only 20% of these samples. DataModels (300K) can identify 50% of validation samples marginally surpassing our performance.

In Fig. 4, we further inspect how well our baseline approach works for each validation sample. We compare the individual estimated support sizes for all 100 samples using our approach versus other baselines. Our results show that for data removal support, across 16% of validation samples, our estimated data removal support is smaller than those of Datamodels (50K). For 44% of the samples our data removal estimates match TRAK and Datamodels (50K). For data mislabel support, our approach finds a smaller support estimate than Datamodels and TRAK for 32% and 79% of the validation samples.

While our baseline approach cannot outperform Datamodels (300K) on data removal, our performance on the data mislabel support is nearly the same. Our baseline approach of using a single self-supervised model can thus serve as a simple, compute, and storage-efficient alternative to estimate data brittleness.

4.3 ImageNet Data Brittleness

In Fig. 5, we show our results for data removal on ImageNet. Our results show that for 4 and 16 of the 30 validation samples our estimated data removal support is less than 16 and 130 training samples respectively. In contrast, TRAK (1) and TRAK (4) do not scale well to ImageNet at all and provide much looser data removal estimates. We again emphasize that even scaling to TRAK with 10 models would require around 400 GB of storage space, by our estimate. This highlights the scalability of our baseline approach where a single self-supervised MoCo backbone can provide more accurate data removal estimates than other existing data attribution methods.

4.4 Transfer to different architecture

Datamodels and TRAK utilize information tied to the model architecture such as gradients or logits from an ensemble of models. However, different neural network architectures are known to exploit similar biases and output similar predictions (Mania et al., 2019; Toneva et al., 2018). In order to better understand how data may be shaping these biases we test how well attribution scores from these approaches transfer to other architectures. Since our approach does not use any information

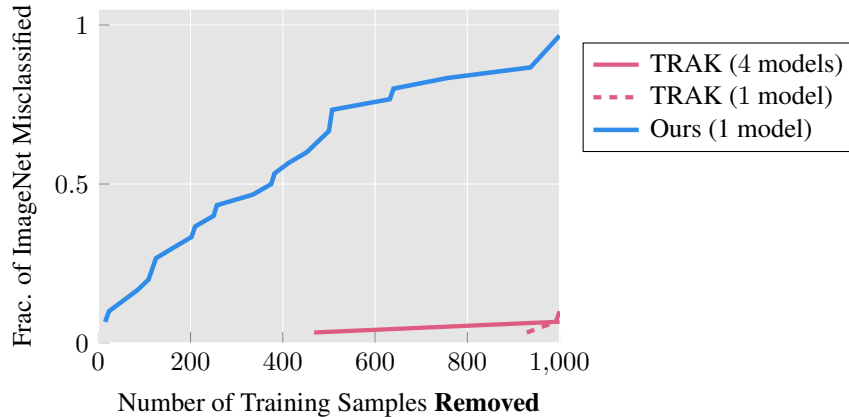


Figure 5: **Our method yields better upper bounds on support size compared to TRAK-4, which requires more storage than the ImageNet dataset itself.** We estimate data removal support for 30 random ImageNet validation samples and plot the CDF of estimates.

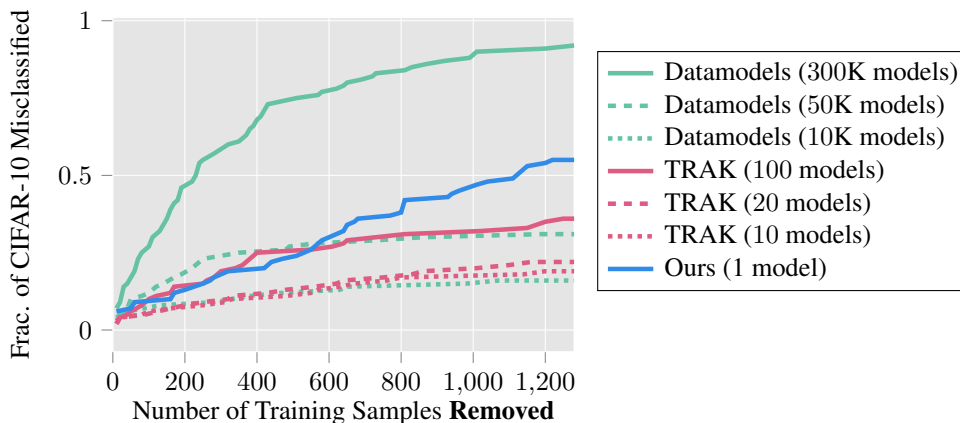


Figure 6: **Our baseline approach is model agnostic and performs well across different architectures.** We evaluate how attribution scores transfer from one architecture transfer to another. We use ResNet-9 scores for TRAK and DataModels and estimate data removal support for MobileNetV2. For our approach, we use the same ResNet-18 backbone.

about the model architecture and only leverages the data, we expect our baseline approach to transfer across different architectures.

In Fig. 6, we compare TRAK, Datamodels, and our attribution scores and evaluate them on a MobileNetV2 architecture (Sandler et al., 2018). The results show that our approach using ResNet-18 continues to predict accurate data removal estimates surpassing TRAK (100) and Datamodels (50K), which suffer a large degradation in performance. Datamodels (300K) also suffer degradation in performance but provide tighter estimates than our approach. This suggests that while simply relying on visual similarity may be useful for efficiently predicting counterfactuals, additional biases within the architecture may also have an influence.

5 Discussion

5.1 Role of Visual Similarity

In Fig. 7, we plot the most similar training images according to Datamodels, TRAK, and our method. Given that our approach relies on comparing MoCo features from the same class as the target image, it makes sense that the closest training images are visually similar. On the other hand, the most similar



Figure 7: **Our attribution method consistently selects the most visually similar training images by design.** In each row, we plot the same target test image (Index 31), followed by ten most similar training images according to each attribution method.

training images found by Datamodels (Ilyas et al., 2022) and TRAK (Park et al., 2023) show more variability. Despite the variability of most similar train images, Datamodels (300K) outperforms all other methods in the counterfactual tasks assessed in Fig. 3, hinting at the importance of additional contributing factors. Still, our method underscores the significant impact of relying solely on visual similarity, essentially showing that a significant fraction of data attribution can be achieved without knowledge of the learning algorithm, based only on knowledge of the training set.

5.2 Other Related Work

Data attribution methods should produce accurate counterfactual predictions about model outputs. Although a counterfactual can be addressed by retraining the model, employing this straightforward approach becomes impractical when dealing with large models and extensive datasets. To address this problem, data attribution methods perform various approximations.

The seminal work on data attribution of Koh & Liang (2017) proposes attribution via approximate *influence functions*. More specifically, Koh & Liang (2017) identify training samples most responsible for a given prediction by estimating the effect of removing or slightly modifying a single training sample. But being a first-order approximation, influence function estimates can vary wildly with changes to network architecture and training regularization (Basu et al., 2021). Nevertheless, approximating influence functions is reasonably inexpensive and has recently also been attempted for multi-billion parameter models Grosse et al. (2023).

Measuring empirical influence has also been attempted through construction of subsets of training data that include/exclude the target sample (Feldman & Zhang, 2020). In a related approach, TracIn (Pruthi et al., 2020) and Gradient Aggregated Similarity (GAS) (Hammoudeh & Lowd, 2022a,b) estimate the influence of each sample in training set S on the test example z_t by measuring the change in loss on z_t from gradient updates of mini-batches. While TracIn can predict class margins reasonably well, the method struggles at estimating data support. Other methods for influence approximation include metrics based on representation similarity (Yeh et al., 2018; Charpiat et al., 2019). Another related line of work has utilized Shapley values to ascribe value to data, but since Shapley values often require exponential time to compute, approximations have been proposed (Ghorbani & Zou, 2019; Jia et al., 2019). In general, there seems to be a recurring tradeoff: methods that are computationally efficient tend to be less reliable, whereas sampling-based approaches are more effective but require training thousands (or even tens of thousands) of models.

6 Conclusion

Data attribution approaches are computationally expensive and can be prone to inaccuracy. While these approaches exhibit promise and capability, their scalability to large-scale models remains uncertain. Our work highlights the importance of visual similarity as a baseline for counterfactual estimation, providing valuable insights into data attribution. Our approach demonstrates scalability and accuracy, particularly in attributions for ImageNet, where it outperforms other state-of-the-art methods while maintaining manageable compute and storage requirements. Remarkably, our approach achieves these results without any reliance on training setup details, target model parameters, or architectural specifics. Our work shows that strong data attribution can be achieved solely based on knowledge of the training set.

7 Acknowledgments and Disclosure of Funding

Vasu Singla was supported in part by the National Science Foundation under grant number IIS-2213335. Pedro Sandoval-Segura is supported by a National Defense Science and Engineering Graduate (NDSEG) Fellowship. Tom Goldstein was supported by the ONR MURI program, the AFOSR MURI program, the National Science Foundation (IIS-2212182), and by the NSF TRAILS Institute (2229885).

References

- Samyadeep Basu, Phil Pope, and Soheil Feizi. Influence functions in deep learning are fragile. In *International Conference on Learning Representations*, 2021. URL <https://openreview.net/forum?id=xHKVVHGDOEk>.
- Emily Black and Matt Fredrikson. Leave-one-out unfairness. In *Proceedings of the 2021 ACM Conference on Fairness, Accountability, and Transparency*, pp. 285–295, 2021.
- Mathilde Caron, Hugo Touvron, Ishan Misra, Hervé Jégou, Julien Mairal, Piotr Bojanowski, and Armand Joulin. Emerging properties in self-supervised vision transformers. In *Proceedings of the IEEE/CVF international conference on computer vision*, pp. 9650–9660, 2021.
- Guillaume Charpiat, Nicolas Girard, Loris Felardos, and Yuliya Tarabalka. Input similarity from the neural network perspective. *Advances in Neural Information Processing Systems*, 32, 2019.
- Ting Chen, Simon Kornblith, Mohammad Norouzi, and Geoffrey Hinton. A simple framework for contrastive learning of visual representations. In *International conference on machine learning*, pp. 1597–1607. PMLR, 2020.
- X Chen, S Xie, and K He. An empirical study of training self-supervised vision transformers. in 2021 *ieee*. In *CVF International Conference on Computer Vision (ICCV)*, pp. 9620–9629.
- Mehdi Cherti, Romain Beaumont, Ross Wightman, Mitchell Wortsman, Gabriel Ilharco, Cade Gordon, Christoph Schuhmann, Ludwig Schmidt, and Jenia Jitsev. Reproducible scaling laws for contrastive language-image learning. In *Proceedings of the IEEE/CVF Conference on Computer Vision and Pattern Recognition*, pp. 2818–2829, 2023.
- Jia Deng, Wei Dong, Richard Socher, Li-Jia Li, Kai Li, and Li Fei-Fei. Imagenet: A large-scale hierarchical image database. In *2009 IEEE conference on computer vision and pattern recognition*, pp. 248–255. Ieee, 2009.
- Keyan Ding, Kede Ma, Shiqi Wang, and Eero P Simoncelli. Image quality assessment: Unifying structure and texture similarity. *IEEE transactions on pattern analysis and machine intelligence*, 44(5):2567–2581, 2020.
- Vitaly Feldman and Chiyuan Zhang. What neural networks memorize and why: Discovering the long tail via influence estimation. *Advances in Neural Information Processing Systems*, 33:2881–2891, 2020.
- Stephanie Fu, Netanel Tamir, Shobhita Sundaram, Lucy Chai, Richard Zhang, Tali Dekel, and Phillip Isola. Dreamsim: Learning new dimensions of human visual similarity using synthetic data, 2023.

- Amirata Ghorbani and James Zou. Data shapley: Equitable valuation of data for machine learning. In *International conference on machine learning*, pp. 2242–2251. PMLR, 2019.
- Priya Goyal, Quentin Duval, Jeremy Reizenstein, Matthew Leavitt, Min Xu, Benjamin Lefaudeux, Mannat Singh, Vinicius Reis, Mathilde Caron, Piotr Bojanowski, Armand Joulin, and Ishan Misra. Vissl. <https://github.com/facebookresearch/vissl>, 2021.
- Jean-Bastien Grill, Florian Strub, Florent Alché, Corentin Tallec, Pierre Richemond, Elena Buchatskaya, Carl Doersch, Bernardo Avila Pires, Zhaohan Guo, Mohammad Gheshlaghi Azar, et al. Bootstrap your own latent—a new approach to self-supervised learning. *Advances in neural information processing systems*, 33:21271–21284, 2020.
- Roger Grosse, Juhan Bae, Cem Anil, Nelson Elhage, Alex Tamkin, Amirhossein Tajdini, Benoit Steiner, Dustin Li, Esin Durmus, Ethan Perez, Evan Hubinger, Kamilë Lukošiuūtė, Karina Nguyen, Nicholas Joseph, Sam McCandlish, Jared Kaplan, and Samuel R. Bowman. Studying Large Language Model Generalization with Influence Functions. *arxiv:2308.03296[cs, stat]*, August 2023. doi: 10.48550/arXiv.2308.03296. URL <http://arxiv.org/abs/2308.03296>.
- Alon Halevy, Peter Norvig, and Fernando Pereira. The unreasonable effectiveness of data. *IEEE intelligent systems*, 24(2):8–12, 2009.
- Zayd Hammoudeh and Daniel Lowd. Identifying a training-set attack’s target using renormalized influence estimation. In *Proceedings of the 2022 ACM SIGSAC Conference on Computer and Communications Security*, pp. 1367–1381, 2022a.
- Zayd Hammoudeh and Daniel Lowd. Training data influence analysis and estimation: A survey. *arXiv preprint arXiv:2212.04612*, 2022b.
- Kazuaki Hanawa, Sho Yokoi, Satoshi Hara, and Kentaro Inui. Evaluation of similarity-based explanations. In *International Conference on Learning Representations*, 2021. URL https://openreview.net/forum?id=9uvhpyQwzM_.
- Kaiming He, X. Zhang, Shaoqing Ren, and Jian Sun. Deep residual learning for image recognition. *2016 IEEE Conference on Computer Vision and Pattern Recognition (CVPR)*, pp. 770–778, 2015. URL <https://api.semanticscholar.org/CorpusID:206594692>.
- Kaiming He, Haoqi Fan, Yuxin Wu, Saining Xie, and Ross Girshick. Momentum contrast for unsupervised visual representation learning. In *Proceedings of the IEEE/CVF conference on computer vision and pattern recognition*, pp. 9729–9738, 2020.
- Edward J Hu, Yelong Shen, Phillip Wallis, Zeyuan Allen-Zhu, Yuanzhi Li, Shean Wang, Lu Wang, and Weizhu Chen. Lora: Low-rank adaptation of large language models. *arXiv preprint arXiv:2106.09685*, 2021.
- Andrew Ilyas, Sung Min Park, Logan Engstrom, Guillaume Leclerc, and Aleksander Madry. Datamodels: Understanding predictions with data and data with predictions. In Kamalika Chaudhuri, Stefanie Jegelka, Le Song, Csaba Szepesvari, Gang Niu, and Sivan Sabato (eds.), *Proceedings of the 39th International Conference on Machine Learning*, volume 162 of *Proceedings of Machine Learning Research*, pp. 9525–9587. PMLR, 17–23 Jul 2022. URL <https://proceedings.mlr.press/v162/ilyas22a.html>.
- Ruoxi Jia, David Dao, Boxin Wang, Frances Ann Hubis, Nick Hynes, Nezihe Merve Gürel, Bo Li, Ce Zhang, Dawn Song, and Costas J Spanos. Towards efficient data valuation based on the shapley value. In *The 22nd International Conference on Artificial Intelligence and Statistics*, pp. 1167–1176. PMLR, 2019.
- Ruoxi Jia, Fan Wu, Xuehui Sun, Jiachen Xu, David Dao, Bhavya Kailkhura, Ce Zhang, Bo Li, and Dawn Song. Scalability vs. utility: Do we have to sacrifice one for the other in data importance quantification? In *Proceedings of the IEEE/CVF Conference on Computer Vision and Pattern Recognition*, pp. 8239–8247, 2021.
- Pang Wei Koh and Percy Liang. Understanding black-box predictions via influence functions. In *International conference on machine learning*, pp. 1885–1894. PMLR, 2017.

- Stephen Kokoska and Daniel Zwillinger. *CRC standard probability and statistics tables and formulae*. Crc Press, 2000.
- Alex Krizhevsky, Geoffrey Hinton, et al. Learning multiple layers of features from tiny images. 2009.
- Guillaume Leclerc, Andrew Ilyas, Logan Engstrom, Sung Min Park, Hadi Salman, and Aleksander Madry. FFCV: Accelerating training by removing data bottlenecks. In *Computer Vision and Pattern Recognition (CVPR)*, 2023. <https://github.com/libffcv/ffcv/>. commit xxxxxxx.
- Zhuoming Liu, Hao Ding, Huaping Zhong, Weijia Li, Jifeng Dai, and Conghui He. Influence selection for active learning. In *Proceedings of the IEEE/CVF International Conference on Computer Vision*, pp. 9274–9283, 2021.
- Scott M Lundberg and Su-In Lee. A unified approach to interpreting model predictions. *Advances in neural information processing systems*, 30, 2017.
- Tomasz Malisiewicz, Abhinav Gupta, and Alexei A. Efros. Ensemble of exemplar-svms for object detection and beyond. In *ICCV*, 2011.
- Horia Mania, John Miller, Ludwig Schmidt, Moritz Hardt, and Benjamin Recht. Model similarity mitigates test set overuse. *Advances in Neural Information Processing Systems*, 32, 2019.
- Sung Min Park, Kristian Georgiev, Andrew Ilyas, Guillaume Leclerc, and Aleksander Madry. Trak: Attributing model behavior at scale. In *International Conference on Machine Learning (ICML)*, 2023.
- Garima Pruthi, Frederick Liu, Satyen Kale, and Mukund Sundararajan. Estimating training data influence by tracing gradient descent. *Advances in Neural Information Processing Systems*, 33: 19920–19930, 2020.
- Mark Sandler, Andrew Howard, Menglong Zhu, Andrey Zhmoginov, and Liang-Chieh Chen. Mobilenetv2: Inverted residuals and linear bottlenecks. In *Proceedings of the IEEE conference on computer vision and pattern recognition*, pp. 4510–4520, 2018.
- Harshay Shah, Sung Min Park, Andrew Ilyas, and Aleksander Madry. Modeldiff: A framework for comparing learning algorithms. In *International Conference on Machine Learning*, pp. 30646–30688. PMLR, 2023.
- Chen Sun, Abhinav Shrivastava, Saurabh Singh, and Abhinav Gupta. Revisiting unreasonable effectiveness of data in deep learning era. In *Proceedings of the IEEE international conference on computer vision*, pp. 843–852, 2017.
- Igor Susmelj, Matthias Heller, Philipp Wirth, Jeremy Prescott, and Malte Ebner et al. Lightly. *GitHub*. Note: <https://github.com/lightly-ai/lightly>, 2020.
- Mariya Toneva, Alessandro Sordoni, Remi Tachet des Combes, Adam Trischler, Yoshua Bengio, and Geoffrey J Gordon. An empirical study of example forgetting during deep neural network learning. *arXiv preprint arXiv:1812.05159*, 2018.
- Chih-Kuan Yeh, Joon Kim, Ian En-Hsu Yen, and Pradeep K Ravikumar. Representer point selection for explaining deep neural networks. *Advances in neural information processing systems*, 31, 2018.
- Richard Zhang, Phillip Isola, Alexei A Efros, Eli Shechtman, and Oliver Wang. The unreasonable effectiveness of deep features as a perceptual metric. In *Proceedings of the IEEE conference on computer vision and pattern recognition*, pp. 586–595, 2018.

A Appendix

A.1 Compute Time and Storage Requirements

For our compute time estimates, we use NVIDIA RTX A6000 GPUs and 4 CPU cores. We describe how we estimate the wall-clock time, and storage requirements for each method below -

- **Datamodels:** We only take into account the storage and compute cost of training models. The additional cost of estimating datamodels from the trained models, requires solving linear regression whose computational costs are negligible compared to training the models. For compute and storage requirement estimates, we train 100 ResNet-9 models on random 50% subsets of CIFAR-10 and extrapolate to estimate the training time and storage required for 10,000 and 50,000 models shown in Section 1.
- **TRAK:** We use the authors’ original code ⁵ to train, and compute the projected gradients for CIFAR-10 using ResNet-9 Models using a projection dimension of 20480. For storage requirements, we take into account storage used by model weights, and the projected gradients. The results in Section 1, show the compute and storage using 10, 20 and 100 models.
- **Ours:** We use Lightly library ⁶ benchmark code to train a MoCo model using a ResNet-18 backbone on CIFAR-10 for 800 epochs. The results in Section 1 show the wall-clock training time for the model, and extracting the features from CIFAR-10 and the storage requirements for model weights.

To calculate the storage requirements, we factor in the storage space necessary for retaining the trained model weights, as they are essential for computing influence on new validation samples across all attribution methods.

A.2 Additional Self-Supervised Features

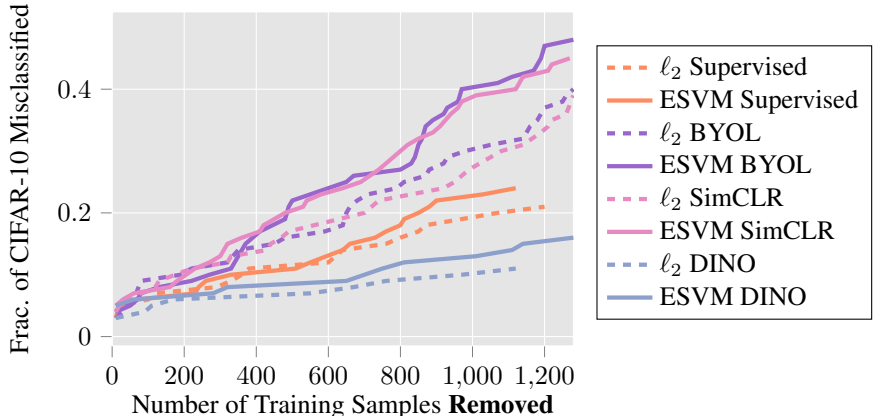


Figure 8: We estimate data removal support for 100 random CIFAR-10 test samples and plot the CDF of estimates.

In addition to utilizing features from MoCo in Section 3, we test our choice of distance function on ResNet-18 features from other self-supervised learning (SSL) methods trained on CIFAR-10. In particular, we evaluate BYOL (Grill et al., 2020), SimCLR (Chen et al., 2020), and DINO (Caron et al., 2021) at estimating data removal support in Fig. 8 and mislabel support in Fig. 9. With the exception of DINO, self-supervised features from BYOL and SimCLR outperform the supervised baseline at estimating data removal support. Additionally, we see that in all cases using ESVM distance is more effective than using ℓ_2 distance to compare features.

⁵<https://github.com/MadryLab/trak>

⁶<https://github.com/lightly-ai/lightly>

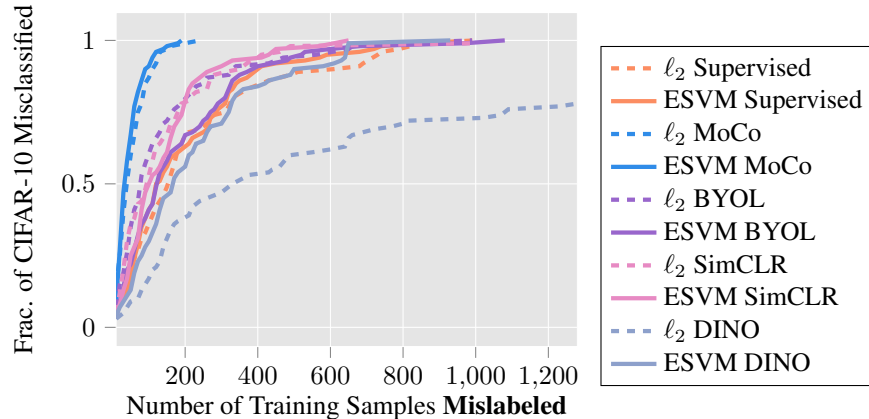


Figure 9: We estimate data mislabel support for 100 random CIFAR-10 test samples and plot the CDF of estimates.

A.2.1 Self-Supervised ImageNet Features

We also consider using ImageNet features from MoCo v3 (Chen et al.) and DINO (Caron et al., 2021) to estimate data removal support in Fig. 10. We use publicly available MoCo v3 and DINO checkpoints from the `vissl` library’s model zoo (Goyal et al., 2021). It is worth noting that this approach places significant emphasis our primary hypothesis, which asserts the importance of visual similarity in data attribution. Utilizing ImageNet features means that the dataset, architecture, and learning objectives are *completely different* from the system we are trying to attribute predictions for: a ResNet-9 trained normally on CIFAR-10. This is in contrast to our main method (ESVM MoCo) which utilizes a ResNet-18 architecture and the CIFAR-10 dataset.

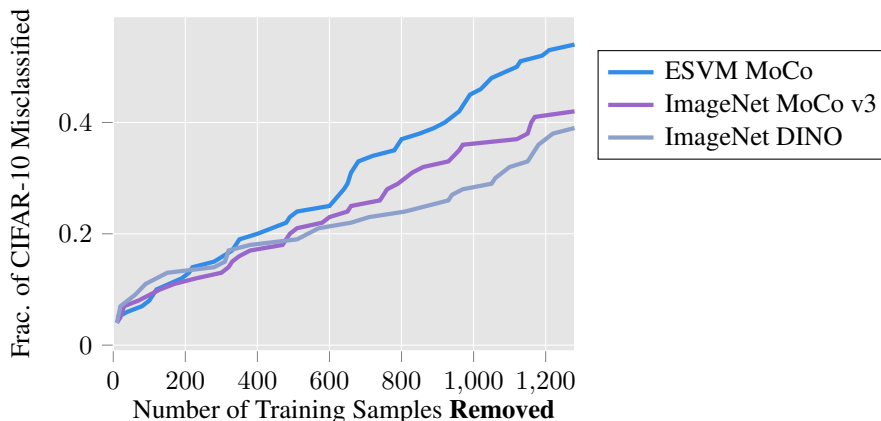


Figure 10: ImageNet features from MoCo v3 and DINO are able to perform very well despite using different architecture (*i.e.* ViT), dataset (*i.e.* ImageNet), and learning objectives (*i.e.* SSL) from the system that we are trying to attribute predictions for: a ResNet-9 trained normally on CIFAR-10.

A.3 Additional Justification for Chosen Subset of Train Images

For a target sample z_t , data attribution approaches rank the training samples based on decreasing order of positive influence on z_t . For our method, a design choice was whether to rank training samples from all classes or from a selected subset of the training data. One reasonable subset was to select training samples from the same class as the target test sample. In Fig. 11, we show that selecting from the same class is more effective when estimating brittleness scores. We maintain this choice for all our experiments.

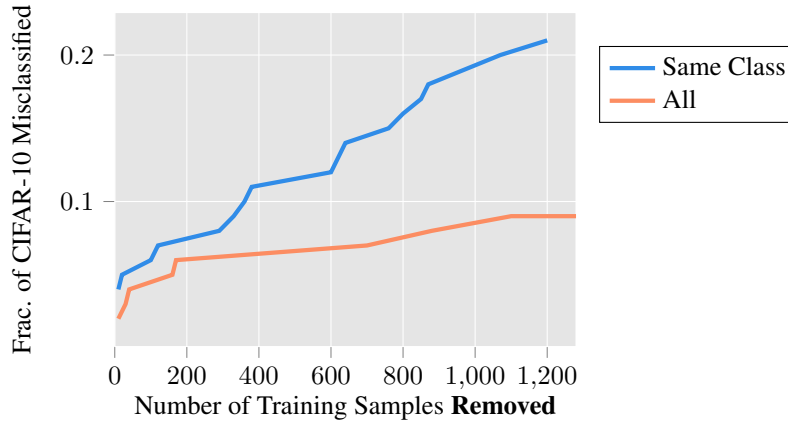


Figure 11: Choosing removal support from all training images is less effective than selecting from the same class as the target image.

A.4 Additional Justification for Distance Function

In Section 3.1, we describe choices for measuring similarity of embeddings: Euclidean distance, cosine distance, and our selection of Exemplar SVM. However, there are a range of other metrics that have been evaluated in prior work. By no means have we exhausted the space of possible metrics, but it relevant to look at recommendations by related work.

A.4.1 Gradient Cosine Similarity

Hanawa et al. (2021) define a set of tests that a similarity metric should satisfy and find that gradient cosine similarity (Grad-Cos) is the only one that passes all tests. Given that Grad-Cos is their overall recommendation for measuring similarity, we evaluate data removal support on CIFAR-10 in Fig. 12. Note that unlike other methods considered, we do not filter images to be of the same class as the target because Grad-Cos already provides a higher ranking to images from the same target class. While we find that Grad-Cos is better than ESVM comparison of supervised features, it still lags behind our main method (ESVM MoCo) from Section 3. Interestingly, in the low data support regime, where fewer than 200 training samples can be removed to misclassify, Grad-Cos is more effective than ESVM MoCo.

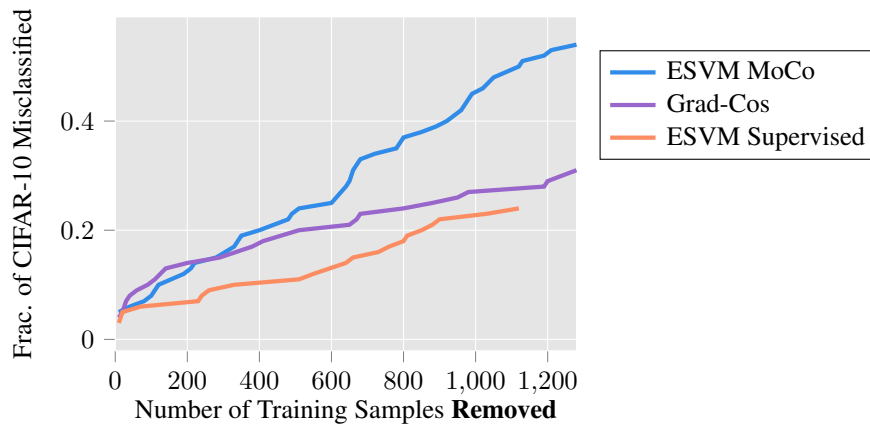


Figure 12: While comparing images with Gradient Cosine Similarity (using a supervised ResNet-9) is better than ESVM on supervised features, it still lags behind our main method (ESVM MoCo).

A.4.2 Human Visual Similarity & DreamSim

Fu et al. (2023) study perceptual metrics and find that large vision models like OpenCLIP (Cherti et al., 2023) and DINO (Caron et al., 2021) are more aligned with human perceptual judgements than other learned metrics like LPIPS (Zhang et al., 2018) and DISTS (Ding et al., 2020). They further improve performance of OpenCLIP and DINO by finetuning with LoRA (Hu et al., 2021) on a dataset of human two-alternative forced choice (2AFC) judgments, called NIGHTS. The best approach on the dataset uses an ensemble of DINO, CLIP, and OpenCLIP features and is called DreamSim. While the ensemble gets 96.2% accuracy on NIGHTS, only utilizing OpenCLIP (with LoRA) gets 95.5% and is $3\times$ faster. Hence, we use this metric in our data removal support evaluation. Here, we also select images from the same training class. In Fig. 13, for every target image, we select the closest training images according to DreamSim to remove. Surprisingly, DreamSim does not improve over our approach using ESVM MoCo.

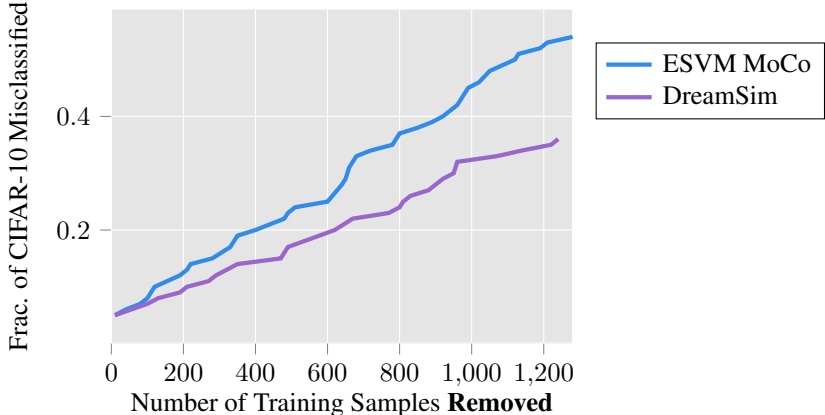


Figure 13: We use DreamSim (OpenCLIP-ViT/32) to select data removal support on CIFAR-10.

A.5 Computing Data Support

We use bisection search to estimate data support. The use of bisection search is supported by the observation that several data attribution approaches are additive (Park et al., 2023), where the importance of a subset of training samples is defined as the sum of each of the samples in the subset. To compute data removal support, we remove M samples (chosen using each attribution method) from the training data and log whether the resulting model misclassifies the target sample. For data mislabeling support, we mislabel M samples (chosen using each attribution method) from the training data and assign a new label corresponding to the highest incorrect logit.

A detailed summary of our bisection search is in Algorithm 1. A key step is $\text{CounterfactualTest}(f, S, I_{\text{attr}}[: M])$ which returns the average classification of N_{test} independent training runs where f_{θ} is trained on the subset $R = \{z_i | z_i \in S \text{ and } i \notin I_{\text{attr}}[: M]\}$. In other words, for computing data removal support, f_{θ} is trained on a subset of S that does not include the first M indices of I_{attr} . For computing mislabeling data support, the only difference is that rather than removing the first M indices of I_{attr} , we relabel those samples with the class of the highest incorrect-class logit, following (Ilyas et al., 2022).

For bisection search across all attribution methods, we use a search budget of 7. For the CIFAR-10 data brittleness metrics, we aggregate predictions over 5 independently trained models. Thus, to evaluate a single validation sample, we train 35 models (7 budget \times 5 models) for a total of 3500 (35 \times 100 samples) models for a data brittleness metric. On ImageNet, we don’t aggregate predictions and only train a single model. Hence, to evaluate a single validation sample on Imagenet, we train 7 models per sample, and a total of 210 models for evaluating a data brittleness metric. Due to the large training cost on ImageNet, we only show results for data removal support. We explicitly point out that these costs are incurred only for analysis of these data attribution methods (see Section 2). Our attribution approach is in comparison, extremely cheap to compute.

Algorithm 1 Bisection Search for Computing Data Support

Input: Target sample, $z_t = (x_t, y_t)$
Input: Training set, S , and a list of top k training set indices I_{attr} ordered by the attribution method $\tau(z, S)$
Input: Model f_θ
Input: Search budget, N_{budget}
Input: Number of times to test classification, N_{test}
Output: N_{support} , size of the smallest training subset $R \subset S$ such that f_θ misclassifies x_t on average

- 1: $L \leftarrow 0$
- 2: $H \leftarrow |I_{\text{attr}}|$
- 3: $M \leftarrow H$
- 4: $C_{\text{avg}} \leftarrow \text{CounterfactualTest}(f, S, I_{\text{attr}}[: M])$
- 5: **if** $C_{\text{avg}} > 0.5$ **then**
- 6: **return** -1 $\triangleright N_{\text{support}}$ is larger than k
- 7: **end if**
- 8: $N_{\text{support}} \leftarrow M$
- 9: **while** $N_{\text{budget}} > 0$ **do**
- 10: $N_{\text{budget}} \leftarrow N_{\text{budget}} - 1$
- 11: $M \leftarrow (L + H)/2$
- 12: $C_{\text{avg}} \leftarrow \text{CounterfactualTest}(f, S, I_{\text{attr}}[: M])$
- 13: **if** $C_{\text{avg}} > 0.5$ **then**
- 14: $L \leftarrow M$
- 15: **else**
- 16: $H \leftarrow M$
- 17: $N_{\text{support}} \leftarrow \min(M, N_{\text{support}})$
- 18: **end if**
- 19: **end while**
- 20: **return** N_{support}

A.6 Linear Datamodeling Score

Let $\tau(z, S) : \mathcal{Z} \times \mathcal{Z}^n \rightarrow \mathbb{R}^n$ be a data attribution method that, for any sample $z \in \mathcal{Z}$ and a training set S assigns a score to every training sample indicating its importance to the model output. Consider a training set $S = \{z_1, z_2 \dots z_n\}$, and a model output function $f_\theta(z)$. Let $\{S_1, \dots, S_m | S_i \subset S\}$ be m random subsets of the training set S , each of size $\alpha \cdot n$ for some $\alpha \in (0, 1)$. The linear datamodeling score (LDS) is defined as:

$$\text{LDS}(\tau(z, S)) = \rho(\{f_{\theta(S_j)}(z) \mid j \in [m]\}, \{\tau(z, S) \cdot \mathbf{1}_{S_j} \mid j \in [m]\}) \quad (1)$$

where ρ denotes Spearman rank correlation (Kokoska & Zwillinger, 2000), $\theta(S_j)$ denotes model parameters after training on subset S_j , and $\mathbf{1}_{S_j}$ is the indicator vector of the subset S_j . Unlike data brittleness metrics, LDS accounts for samples with positive as well as negative influence.

To compute LDS scores, for our model output function $f_\theta(z)$, we use the correct class margin. This is defined as:

$$f_\theta(z) = (\text{logit for correct class}) - (\text{highest incorrect logit})$$

Our approach cannot directly be applied to compute LDS scores, as for a validation sample z_t we only focus on training samples with the most positive impact. We propose a simple modification to our approach. We assign a score to each training data based on the inverse of signed l_2 distance. The sign is based on whether the label for the training sample matches z_t . We then threshold our scores, such that all scores beyond the top-5% are zero leading to sparser attribution scores. The sparsity prior has been shown to be effective for data attribution (Ilyas et al., 2022; Park et al., 2023).

In Table 1, we present a comparison of LDS scores using our baseline approach, TRAK and Datamodels. Although our baseline was not initially designed for direct LDS score approximation, a simple adaptation demonstrates comparable performance to TRAK (5) on CIFAR-10. TRAK with a larger ensemble of models can achieve higher LDS scores. The Datamodels framework was optimized

| | Models Used | LDS Scores |
|------------|-------------|------------|
| Datamodels | 300,000 | 0.56 |
| | 50,000 | 0.43 |
| | 10,000 | 0.24 |
| TRAK | 100 | 0.22 |
| | 20 | 0.15 |
| | 10 | 0.12 |
| | 5 | 0.08 |
| Ours | 1 | 0.08 |

Table 1: We compare LDS scores for our approach with other baselines on CIFAR-10. Our proposed approach can perform equivalent to TRAK with 5 models.

for this objective and trained as a supervised learning task, using tens of thousands of models. Hence, it achieves a better correlation with LDS.

It is important to highlight that while Datamodels and TRAK outperform our baseline in terms of LDS with extensive model ensembles, this metric provides limited insights into understanding machine learning models. Our baseline approach excels in data brittleness metrics, offering a faithful representation of which training samples provide the most positive influence for a test sample.